ARMY RESEARCH LABORATORY

Synthetic Discriminant Function Performance Versus Filter Count

Michael J. Vrabel

ARL-TN-157   April 2000

DTIC QUALITY INSPECTED 2

20000516 035

Army Research Laboratory

Adelphi, MD 20783-1197

Synthetic Discriminant Function Performance Versus Filter Count

Michael J. Vrabel

Sensors and Electron Devices Directorate

Abstract

The relationship between performance and filter count is examined for a synthetic discriminant function-based target-detection algorithm.

Contents

Figures

1. Introduction

This report examines the relationship between the performance of the synthetic discriminant function (SDF) approach to automatic target recognition (ATR) and SDF filter count. The SDF approach to ATR is relatively mature, with much research published on various aspects of this concept appearing in the literature [1–7]. While a classification capability presently exists, I do not include it in this report. Consequently, this report is to be restricted to target detection only.

2. Clustering

To develop a set of SDF filters, one must have a reasonable method for organizing target images (the basis for the filters) based on some measure of target image similarity. For present purposes, all images are masked scene size (128 × 128 pixels) representations with varying-sized centered targets. One obvious and reasonable basis for clustering images is the Euclidean distance between images in gray-scale pixel space. The images used to construct the filters can be represented by a set of reference vectors, one for each filter, that minimizes the following cost function:

$$\varepsilon = \sum_i \sum_{x \in \xi_i} \| x - c_i \|^2 ,\qquad (1)$$

where x is an image vector, c_i is a reference vector for cluster ξ_i, and $x \in \xi_i$ if

$$\| x - c_i \| < \| x - c_j \|, j \neq i .\qquad (2)$$

An obvious approach to a solution is the well-known k-means algorithm [8]. Traditional k-means suffers from problems addressed by a number of authors. The algorithm to be used in this report is the latest and probably the best iteration on this concept [9]. It is referred to as "optimal adaptive k-means." In adaptive k-means, the k-means uses an iterative approach to finding a set of optimum reference vectors. An updated vector is computed as

$$c_{k.T+1} = c_{k.T} + M_k \nu (x_T - c_{k.T}) ,\qquad (3)$$

where ν is a constant governing the learning rate and M_k is defined as

$$M_k = 1 \quad \text{if} \quad v_k(\| x - c_k \|^2) \leq v_i(\| x - c_i \|^2) \quad i \neq k ;\qquad (4)$$

$$M_k = 0 \quad \text{otherwise.}$$

To obtain the within-region variation v_k, one calculates

$$v_{k.T+1} = \alpha v_{k.T} + (1 - \alpha)(M_k \| x_T - c_{k.T} \|^2) ,\qquad (5)$$

with α as a constant selected to be slightly less than 1.

One potential problem suffered by all k-means algorithms is the inability to define initial reference vectors (with its potential consequence on finding

a globally optimum solution). Rather than selecting initial reference vectors randomly, I used a recurrent neural network to perform this task. It has been shown that the Hopfield neural network [10] can be used to solve various problems in optimization [11–14]. Its properties are detailed elsewhere [10]. In the following, I briefly summarize its attributes. The asynchronously updated state of each neural network node is

$$V_n = \Gamma \left(\sum_{m=1}^{N} W_{nm} V_m \right),$$ (6)

where

V_m = present state of node m,

N = node count,

W_{nm} = nodes n to m weights, and

Γ = a hard thresholding function. If the following restrictions are imposed upon the weights,

$$W_{nm} = W_{mn} \text{ and}$$
$$W_{mm} = 0,$$

then an energy function can be associated with the network (assuming a zero externally applied threshold):

$$E = -1/2 \sum_{n=1}^{N} \sum_{m=1}^{N} W_{nm} V_n V_m .$$ (7)

An asynchronous network update guarantees an eventual settling into a final invariant state for all nodes—a state representing either a global or local energy minimum. Note from equations (6) and (7) that a two-population distribution will be selected that minimizes the absolute values of the weights within each population and maximizes them between populations. The resultant vectors have just the attributes required for initializing k-means. In this instance, the weights are equated with an average difference in gray-scale pixel values among the filter-generating images. The neural network divides the image population into two clusters. To increase the population cluster count, one determines the standard deviation of each cluster and subdivides the cluster with the largest deviation using, once more, the Hopfield neural network. In this way, the initial population can be divided into as many clusters as desired.

3. Results

The purpose of this work is to explore the relationships among four significant variables: (1) filter count, (2) false-alarm rate, (3) target-detection rate, and (4) SDF threshold. To test the performance of the SDF algorithm as a function of filter count, I modified the original code* to allow a filter count independent of the target count. I then ran the code with the chosen filter population and combined the results for each filter. The output from each filter was examined for peaks in the response as per standards built into the SDF code, and the magnitude and location of each peak were stored for a maximum of the 60 largest peaks. This meant that a maximum of 480 peak responses could be stored for the maximum tested filter count of eight for each analyzed scene. All peak responses for a given filter set were ordered by magnitude, and the resultant data set was scanned starting at the maximum response. A circle of one of three chosen radii (3, 5, and 10 pixels) was centered on the location of the given peak, and the peaks within the circle were combined two different ways. The first approach was to consider any peak falling within a given circle as coincident with the main peak of that circle with the consequence that all lesser peaks were eliminated from the peak list.

The second approach was to define a location for the within-circle response by averaging the weighted locations of all peaks within the circle. The weighting factor was just the location peak response. Again, the ancillary within-circle peaks were eliminated from the peak response set. After comparing both approaches, I found little difference in the final results. Thus, all subsequent results are to be given for the first (and simpler) approach. A target was considered detected if its location fell within a radius of the peak response location as defined previously. Similarly, when consolidating all background hits falling within the preceding defined circle into a consequent single hit, I assumed that all hits within the circle were detecting the same false background attribute.

Figure 1 contains four examples of the target-containing scenes used to examine filter performance. The images in these scenes were selected from the beginning, middle, and end of the test sequence and represent the whole data set. The crosshairs are centered on the targets. The images are in an as-given state, with no rescaling or image renormalization. A narrow band

---

*The original version of the SDF code was written by Lipchen (Alex) Chan of ARL.

Figure 1. Example scenes with targets indicated by crosshairs.
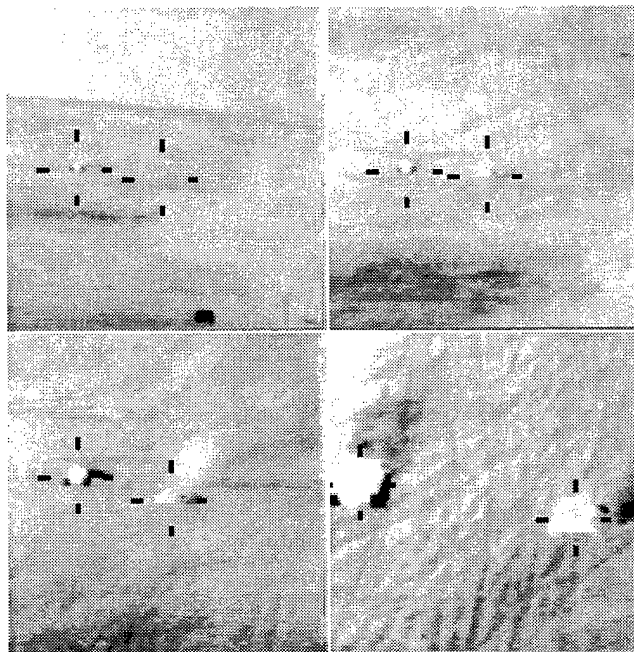
of pixels appearing about the perimeter of some of the images has an intensity distribution unlike the rest of the scene. For this reason, I discarded all peak responses occurring within six pixels of the scene perimeter. All images are 128 × 128 pixels and the test sequence comprises 236 scenes, each containing two target images. Additional details about each of these two images and the images used to create the filter sets are given in the appendix.

False alarm versus target-detection rates are given in figure 2. The graph legend identifies the number of filters for a target-detection rate radius (as previously noted) of 3, 5, and 10 pixels. In general, the larger the filter count the poorer the performance. Figure 3 is the background and target performance as a function of threshold. As can be seen, the relatively modest target-detection rate improvement with filter count increase is more than offset by the corresponding increase in false alarms.

The SDF model has a number of desirable attributes:

- It readily adapts to a changing target environment.

- It appears to extract even low-quality images.

- Speed of execution appears to make the SDF model amenable to a real-time implementation.

5

Figure 2. Target-detection rate versus false alarms. Legends show filter counts of 1 to 4, 6, and 8 and three circle radii (a) 3, (b) 5, and (c) 10 pixels.

6
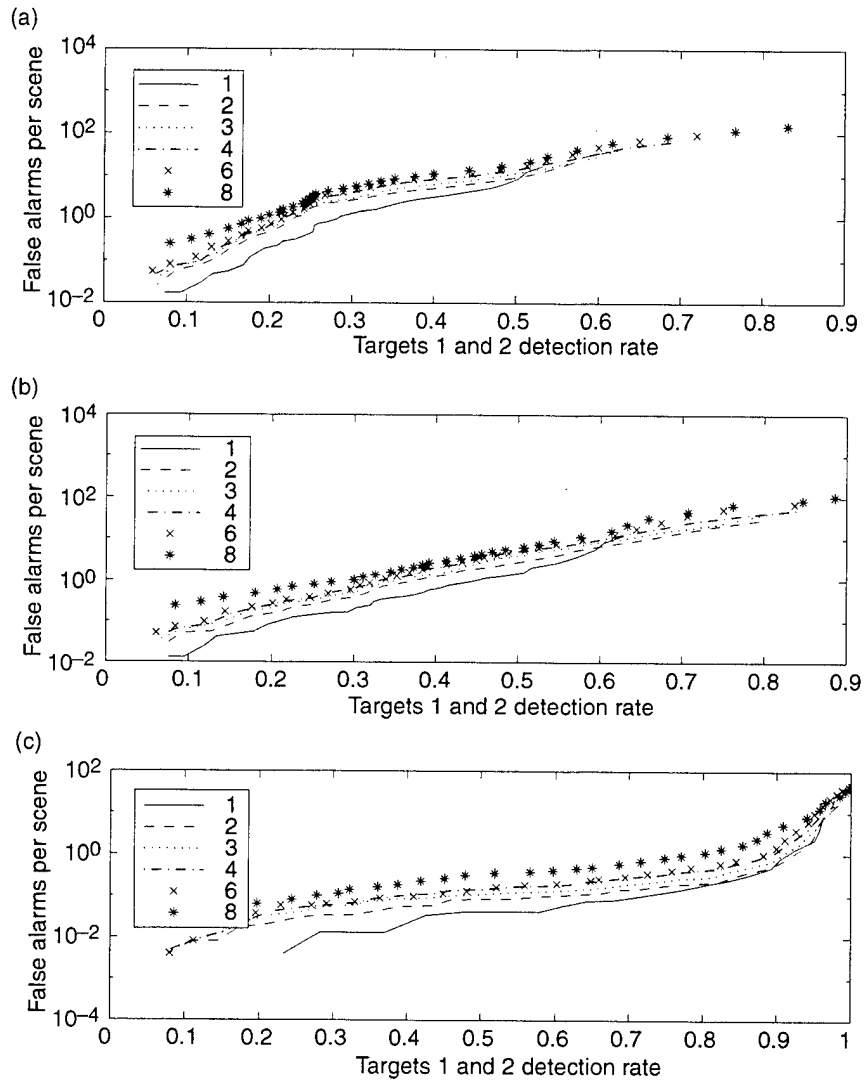
Figure 3. Threshold versus
false-alarm and
target-detection rates.
Legends show filter counts
of 1, 2, 4, and 8 and circle
radii of 3 and 5 pixels.
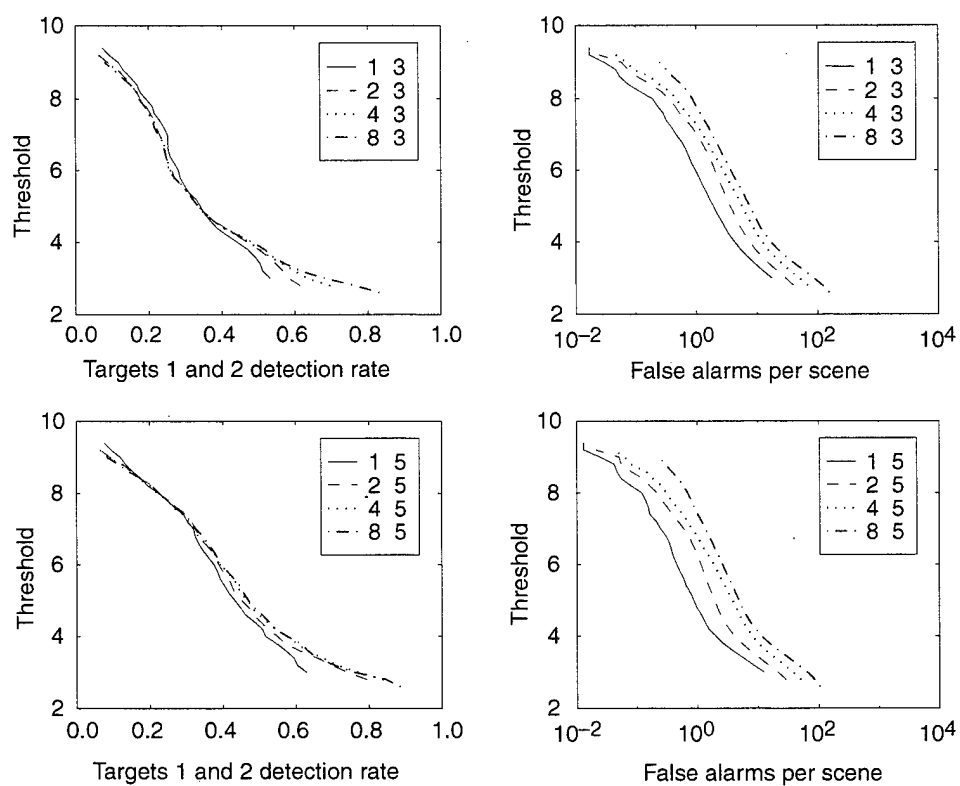
4. Conclusion

A clustering algorithm was developed to optimally organize a set of correlation filter images for an SDF-based target-detection algorithm into one through eight populations. The resultant set of one through eight filters was tested (target-detection versus false-alarm rate) with the SDF algorithm. It was demonstrated that for the test population of target-containing scenes, the optimum SDF filter count is one.

8

References

1. A. Mahalanobis, "Special section on correlation pattern recognition," ed., *Opt. Eng.* **36**, 10 (1997).

2. A. Mahalanobis, B.V.K. Vijaya Kumar, and S.R.F. Sims, "Distance-classifier correlation filters for multiclass target recognition," *Appl. Opt.* **35** (1996), 3127–3133.

3. D. L. Flannery, "Optimal trade-off distortion-tolerant constrained-modulation correlation filters," *J. Opt. Soc. Am.* **A12** (1995), 66–72.

4. A. Mahalanobis, B.V.K. Vijaya Kumar, S. Song, S.R.F. Sims, and J. F. Epperson, "Unconstrained correlation filters," *Appl. Opt.* **33** (1994), 3751–3759.

5. B.V.K. Vijaya Kumar, "Tutorial survey of composite filter designs for optical correlators," *Appl. Opt.* **31** (1992), 4773–4801.

6. B.V.K. Vijaya Kumar, A. Mahalanobis, S. Song, S.R.F. Sims, and J. F. Epperson, "Minimum squared error synthetic discriminant functions," *Opt. Eng.* **31** (1992), 915–922.

7. C. F. Hester and D. Casasent, "Multivariant technique for multiclass pattern recognition," *Appl. Opt.* **19** (1980), 1758–1761.

8. S. P. Lloyd, "Least squares quantization in PCM, Bell Laboratories Internal Technical Report," *IEEE Trans. Inf. Theory* **IT-28:2** (1957), 1982.

9. C. Chinrunggrueng and C. H. Sequin, "Optimal adaptive k-means algorithm with dynamic adjustment of learning rate," *IEEE Trans. Neural Networks* **6** (1995), 157–169.

10. J. J. Hopfield, "Neural networks and physical systems with emergent collective computational abilities," *Proc. Nat. Acad. Sci.* **79** (1982), 2554–2558.

11. J. J. Hopfield and D. W. Tank, "Neural computation of decision in optimization problem," *Biol. Cybern.* **52** (1985), 141–152.

12. S. Cavalieri, A. Di Stefano, and O. Mirabella, "Optimal path determination in a graph by Hopfield neural network," *Neural Networks* **7** (1994), 397–404.

13. M. J. Vrabel, "Image edge detection with a recurrent neural network," Proc. SPIE **2760** (1996).

14. M. J. Vrabel, "Neural network-based segmentation," *Proc. IASTED* (SIP'96) (1996), 173–177.

Appendix. Attributes—Image Set and SDF Codes

All filters were constructed from an image data set provided by the U.S. Army Aviation and Missile Command (AMCOM). This set contained 716 images and comprises the following images: l1815041_r1.apc through l1815226_r1.apc and l1816053%s through l1816288%s, where %s is one of the following: .m60, .tnk, _r1.m60, or _r1.tnk.

The SDF-based ATR algorithm was tested on the following set of 236 AMCOM-provided scenes: L1816S00053_r1.bin through L1816S00288_ri.bin. Each scene contained two target images: the M60 and tnk.

The following is a flowchart of the codes used for this study, along with the files generated by each code. This chart is followed by a description of the contents of each output file. All source code is available upon request.

- **filter_cluster.c**
outputs: ↓

    1.:   diagnostics

    2.:   distance_matrix

    3.:   hopfield_clusters

    4.:   vector%d.dat

    5.:   matrix

    6.:   merged_file

- **make_list.c**
outputs: ↓

    7.:   detect_list%d → mv to: test.list

- **sdf.c** → a.out -bd 1
  (change value NOBJECT to filter count)
outputs: ↓

    8.:   test.dfil

- **make_frame_list.c**
outputs: ↓

    9.:   test.list

- **sdf.c** → a.out -td 1
outputs: ↓

    10.: detection.dat

    11.: images.dat

    12.: sdf_output.dat

- **sdf_imaging.c**
outputs: ↓

    13.: scene.dat → MATLAB$^{\text{TM}}$ imagery

- **sdf_evaluate.c**
outputs: ↓

    14.: results.%d.%d.dat

- **plot_maker.c** → MATLAB 2D curves

Output file contents.

diagnostics: Contains a description of the code performance at every 50 iterations for each cluster. This includes (1) $(c_{k,T} - c_{k,i})/c_{k,i}$, where i refers to the initial value of the reference vector; (2) the filter image population count for each cluster; and (3) the within-region variation v_k.

distance_matrix: Contains the gray-scale distance matrix for the 716 filter images.

hopfield_clusters: Assigns each of the 716 filter images to its appropriate cluster for filter counts of 1 through n, with n nominally assigned the value 8. This is for the Hopfield clustering model.

vector%d.dat: Contains the 128 × 128 final reference vectors for a cluster count defined by %d.

matrix: Is averaged distances between the Hopfield cluster populations for cluster count of 1 through, nominally, 8.

merged_file: For the 716 filter images, contains in column format the cluster membership for a 1 through 8 cluster population, along with the image ID.

detect_list: Contains from merged_file the population for a selected cluster count along with the full paths to the individual images.

test.dfil: Is the filter set generated by sdf.c to be used by the detection function of the aforementioned code.

test.list: Contains table of image file names of scenes to be analyzed by the SDF code detector.

12

detection.dat: Contains the detector response map for a limited number of scenes along with the corresponding target locations.

images.dat: Contains a limited number of the unprocessed scenes used as input to the detector.

sdf_output.dat: Lists the locations of all targets on all scenes passed through the detector along with the top 60 peaks of the detector's output for each filter.

scene.dat: Contains a square array of image pixels composed of either (multiple) unprocessed scenes or the output of the detector with all targets indicated with crosshairs and in a MATLAB compatible format.

results.%d.%d.dat: Is in a four-column format: first column are threshold values; second column, corresponding first target-detection rate; third column, the second target-detection rate, and fourth column, the per scene background hit count. The first %d is the filter count and the second %d is the aforementioned radius value.

Distribution

Admnstr
Defns Techl Info Ctr
Attn DTIC-OCP
8725 John J Kingman Rd Ste 0944
FT Belvoir VA 22060-6218

Ofc of the Secy of Defns
Attn ODDRE (R&AT)
The Pentagon
Washington DC 20301-3080

Ofc of the Secy of Defns
Attn OUSD(A&T)/ODDR&E(R) R J Trew
3080 Defense Pentagon
Washington DC 20301-7100

AMCOM MRDEC
Attn AMSMI-RD W C McCorkle
Attn AMSMI-RD-MG-IP R Sims
Redstone Arsenal AL 35898-5240

CECOM
Attn PM GPS COL S Young
FT Monmouth NJ 07703

Dir for MANPRINT
Ofc of the Deputy Chief of Staff for Prsnnl
Attn J Hiller
The Pentagon Rm 2C733
Washington DC 20301-0300

Night Vsn & Elect Sensors Dir
Attn AMSEL-RD-NVOD L Garn
10221 Burbeck Rd Ste 430
FT Belvoir VA 22060-5806

US Army ARDEC
Attn AMSTA-AR-TD M Fisette
Bldg 1
Picatinny Arsenal NJ 07806-5000

US Army Info Sys Engrg Cmnd
Attn ASQB-OTD F Jenia
FT Huachuca AZ 85613-5300

US Army Natick RDEC
Acting Techl Dir
Attn SSCNC-T P Brandler
Natick MA 01760-5002

US Army Simulation, Train, & Instrmntn
  Cmnd
Attn J Stahl
12350 Research Parkway
Orlando FL 32826-3726

US Army Tank-Automtv Cmnd Rsrch, Dev, &
  Engrg Ctr
Attn AMSTA-TR J Chapin
Warren MI 48397-5000

US Army Train & Doctrine Cmnd
Battle Lab Integration & Techl Dirctrt
Attn ATCD-B J A Klevecz
FT Monroe VA 23651-5850

US Military Academy
Mathematical Sci Ctr of Excellence
Attn MDN-A LTC M D Phillips
Dept of Mathematical Sci Thayer Hall
West Point NY 10996-1786

Nav Surface Warfare Ctr
Attn Code B07 J Pennella
17320 Dahlgren Rd Bldg 1470 Rm 1101
Dahlgren VA 22448-5100

DARPA
Attn S Welby
3701 N Fairfax Dr
Arlington VA 22203-1714

Hicks & Associates Inc
Attn G Singley III
1710 Goodrich Dr Ste 1300
McLean VA 22102

Palisades Inst for Rsrch Svc Inc
Attn E Carr
1745 Jefferson Davis Hwy Ste 500
Arlington VA 22202-3402

US Army Rsrch Ofc
Attn AMSRL-RO-D JCI Chang
Attn AMSRL-RO-EN W Bach
PO Box 12211
Research Triangle Park NC 27709

Distribution (cont'd)

US Army Soldier & Biol Chem Cmnd
Dir of Rsrch & Techlgy Dirctrt
Attn SMCCR-RS I G Resnick
Aberdeen Proving Ground MD 21010-5423

TECOM
Attn AMSTE-CL
Aberdeen Proving Ground MD 21005-5057

US Army Rsrch Lab
Attn AMSRL-DD J M Miller
Attn AMSRL-CI-AI-A Mail & Records Mgmt

US Army Rsrch Lab (cont'd)
Attn AMSRL-CI-AP Techl Pub (3 copies)
Attn AMSRL-CI-LL Techl Lib (3 copies)
Attn AMSRL-IS-EP P Gillespie
Attn AMSRL-SE J Pellegrino
Attn AMSRL-SE-SA J Eicke
Attn AMSRL-SE-SE M Vrabel (5 copies)
Adelphi MD 20783-1197

REPORT DOCUMENTATION PAGE

Public reporting burden for this collection of information is estimated to average 1 hour per response, including the time for reviewing instructions, searching existing data sources, gathering and maintaining the data needed, and completing and reviewing the collection of information. Send comments regarding this burden estimate or any other aspect of this collection of information, including suggestions for reducing this burden, to Washington Headquarters Services, Directorate for Information Operations and Reports, 1215 Jefferson Davis Highway, Suite 1204, Arlington, VA 22202-4302, and to the Office of Management and Budget, Paperwork Reduction Project (0704-0188), Washington, DC 20503.

1. AGENCY USE ONLY *(Leave blank)*	2. REPORT DATE April 2000	3. REPORT TYPE AND DATES COVERED Final, 1 Oct 98 to 30 Sept 99

4. TITLE AND SUBTITLE Synthetic Discriminant Function Performance Versus Filter Count

5. FUNDING NUMBERS

DA PR: AH16

PE: 62120A

6. AUTHOR(S) Michael J. Vrabel

7. PERFORMING ORGANIZATION NAME(S) AND ADDRESS(ES)
U.S. Army Research Laboratory
Attn: AMSRL-SE-SE   email: vrabel@arl.mil
2800 Powder Mill Road
Adelphi, MD 20783-1197

8. PERFORMING ORGANIZATION REPORT NUMBER
ARL-TN-157

9. SPONSORING/MONITORING AGENCY NAME(S) AND ADDRESS(ES)
AMCOM*
Redstone Arsenal, AL 35898-5240

10. SPONSORING/MONITORING AGENCY REPORT NUMBER

11. SUPPLEMENTARY NOTES   *Also sponsored by the U.S. Army Research Laboratory.
ARL PR: 9NE4MM
AMS code: 622120.H16

12a. DISTRIBUTION/AVAILABILITY STATEMENT Approved for public release; distribution unlimited.	12b. DISTRIBUTION CODE

13. ABSTRACT *(Maximum 200 words)*
The relationship between performance and filter count is examined for a synthetic discriminant function-based target-detection algorithm.

14. SUBJECT TERMS SDF, correlation filters, automatic target recognition	15. NUMBER OF PAGES 23
	16. PRICE CODE

17. SECURITY CLASSIFICATION OF REPORT Unclassified	18. SECURITY CLASSIFICATION OF THIS PAGE Unclassified	19. SECURITY CLASSIFICATION OF ABSTRACT Unclassified	20. LIMITATION OF ABSTRACT UL

NSN 7540-01-280-5500